Electronic Supplementary Material (ESI) for ChemComm.

A Ni(I)Fe(II) analogue of the Ni-L state of the Active Site of the [NiFe] Hydrogenases

C. U. Perotto, G. Marshall, G. J. Jones, E. S. Davies, W. Lewis, J. McMaster and M. Schröder.

Electronic Supporting Information

Experimental

General experimental procedures. Elemental analyses were carried out by the London Metropolitan University (Carlo Erba CE1108 Elemental Analyser). Infrared spectra were recorded on a Nicolet Avatar 360 FTIR spectrometer and solution infrared spectra were recorded using sealed solution cells with either CaF_2 or KBr windows. NMR spectra were recorded either on a Bruker DPX300, DPX400 or AV400 spectrometers. Mass spectra (ESI) were recorded by the Mass Spectrometry Service at the University of Nottingham. Electrochemical measurements were made using an Eco Chemie Autolab PGSTAT20 potentiostat. All solutions were purged with a stream of Ar prior to use. Cyclic voltammograms were performed using a three-electrode system, with a glassy carbon working electrode (6.7 mm diameter), a Pt wire secondary electrode and a saturated calomel reference electrode. All potentials are referenced to the Fc^+/Fc couple that was used as an internal standard. Cyclic voltammograms were recorded for solutions of compound (*ca.* 1 mM) with $[N^nBu]_4[BF_4]$ (0.4 M) as supporting electrolyte. Coulometric measurements were performed using an H-cell at 273 K in CH_2Cl_2 containing $[N^nBu_4][BF_4]$ (0.4 M); the cell consisted of a Pt/Rh gauze basket working electrode separated by a glass frit from a Pt/Rh gauze secondary electrode. The saturated calomel reference electrode was placed at the centre of the working electrode and the solution was stirred rapidly during electrolysis using a magnetic stirring bar. The UV-visible spectroelectrochemical experiments were carried out at 273 K or 243 K with an optically transparent electrode mounted in a modified quartz cuvette with an optical pathlength of 0.5 mm. A three-electrode configuration consisting a Pt/Rh gauze working electrode, a Pt wire secondary electrode (in a fritted PTFE sleeve) and a saturated calomel electrode, chemically isolated from the test solution via a bridge tube containing electrolyte solution and terminated in a porous frit, was used in the cell. The potential at the working electrode was controlled by a Sycopel Scientific Ltd. DD10M potentiostat. The UV-visible spectra were recorded on a Perkin Elmer Lambda 16 spectrophotometer. The spectrometer cavity was purged with N_2 and temperature control at

the sample was achieved by flowing cooled N_2 across the surface of the cell. X-band EPR spectra were recorded on a Bruker EMX spectrometer at the University of Nottingham. The simulations of the EPR spectra were performed using the Bruker WINEPR SimFonia package.

Synthesis and materials. All reactions and manipulations were carried out under an Ar atmosphere using standard Schlenk techniques. Unless otherwise stated, the reagents were used as received from the suppliers (Sigma-Aldrich, Acros Organic and Fluka). [Ni(L^1)], was prepared according to literature procedures.[1] Solvents were dried and degassed following standard procedures and stored under Ar in Young's ampoules over molecular sieves (pore size 4 Å).

[Ni(L^1)Fe(^{t}BuNC)$_4$](PF$_6$)$_2$ ([1](PF$_6$)$_2$). A solution of [Ni(L^1)] (153 mg, 0.5 mmol) in MeCN (5 ml) was added to a solution of $FeCl_2$ (63 mg, 0.5 mmol) in MeCN (5 ml). After 1 h ^{t}BuNC (0.25 ml, 2 mmol) was added resulting in the formation of a red solution. After 1 h the solution was filtered and the volatiles were removed under reduced pressure to afford a red solid. The red solid was dissolved in H_2O (10 mL) and the addition of NH_4PF_6 (815 mg , 5 mmol) to this solution resulted in the immediate precipitation of [Ni(L^1)Fe(^{t}BuNC)$_4$](PF$_6$)$_2$ that was isolated by filtration and washed with water. The solid was extracted with MeCN and the solution evaporated to dryness under vacuum to afford a red-orange solid (380 mg, 78%). ESI-MS: 839.2659 m/z $[M+PF_6]^+$ (calc 839.2665 m/z). ^{31}P-NMR(162 MHz, CD_3CN, 298K): δ ppm -144.57 (m, PF_6). ^{1}H-NMR (300 MHz, Acetonitrile-d_3): δ ppm 1.43 (t, J = 7.11 Hz, 6 H, -CH_2CH_3) 1.46 - 1.61 (m, 27 H, ^{t}*Bu*NC) 1.79 - 1.87 (m, 9 H, ^{t}*Bu*NC) 1.97 - 2.04 (m, 2 H, L^1 CH_2) 2.08 - 2.20 (m, 2 H, L^1 CH_2) 2.45 - 2.58 (m, 2 H, L^1 CH_2) 2.63 - 2.79 (m, 4 H, L^1 CH_2) 2.81 - 3.09 (m, 6 H, L^1 CH_2). IR (MeCN) ν_{max}/cm^{-1} (NC) 2202 (s), 2170 (s), 2161 (s), 2145 (s) cm^{-1}. Elemental analysis, found (calc. for $C_{31}H_{60}F_{12}Fe_1Ni_1N_6P_2S_2$): C, 37.83 (37.78); H, 6.27 (6.14); N, 8.45 (8.53)%. Single crystals of [**1**](PF$_6$)$_2$·MeCN suitable for XRD experiments were obtained by the slow diffusion of Et_2O into a MeCN solution of [**1**](PF$_6$)$_2$ at 4°C over 21 days.

Reduction of [1](PF$_6$)$_2$ and the subsequent reaction with CO. Solid [Cp_2^*Co] (6 mg, 18 μmol) was added a solution of [**1**](PF$_6$)$_2$ (15 mg, 15.2 μmol) in MeCN (5 mL) and the solution was cooled to 243 K. After 15 min the colour of the reaction mixture turned from

light orange to deep brown-red. The IR spectrum of the mixture showed new bands at 2163, 2129, 2216 and 1867 $cm^{-1,}$ indicative of the formation of the reduced species $[\mathbf{1}]^+$. The atmosphere in the reaction vessel was changed from Ar to CO and the solution was saturated by bubbling CO gas through the solution for 5 min. The colour of the reaction mixture turned light brown-orange within 10 min. The IR spectrum of the reaction mixture showed bands at 1921 and 1878 cm^{-1} together with several bands in the 2220-1980 cm^{-1} region. No residual bands for the $[\mathbf{1}]^+$ were observed which indicated full reaction of $[\mathbf{1}]^+$ with CO. The same result is obtained when the reduction of $[\mathbf{1}]^{2+}$ with $[Cp_2^*Co]$ is performed entirely under a CO atmosphere.

Computational details All DFT calculations were performed using Gaussian 03.[2] Geometry optimizations and IR spectra were calculated using the BP86 functional.[3,4] Single point electronic calculations were performed using the three-parameter hybrid exchange functional[5] and the Lee-Yang-Parr correlation function[6] (B3LYP). For geometry optimizations the basis set was an adapted version of that used by Hall *et al.*.[7] The Ni and Fe atoms were described by the Hay and Wadt basis set[8] with effective core potential (ECP); the 4p orbitals in the ECP basis set were replaced by optimized (41) split valence functions from Couty and Hall[9] and augmented by an f-polarization function.[10] The standard LANL2DZ basis set was augmented with a d-polarization and p-diffuse function for S.[11] The 6-31G(d,p)[12] basis set was used for the C and N atoms of the ligands while the STO-3G was employed for the H atoms. After optimization a frequency analysis was performed to confirm that the stationary point was found to be a minimum on the potential energy surface. For electronic properties the all-electron Wachters (+f) basis set was used for Ni and Fe while the C, H, S and N atoms were described with the 6-311G(d,p) basis set.[13–15] For $[\mathbf{1}]^+$, a restricted open-shell calculation (RO) with the B3LYP functional was used to minimize spin contamination. Unrestricted calculations of the spin Hamiltonian parameters (Table S2) for $[\mathbf{1}]^+$ used the BP86 functional, the all-electron Wachters (+f) basis set for Ni and Fe, the EPRII basis set for the C, H and N atoms and the 6-311G(d,p) basis set for S.[13-16] Unrestricted calculations of the spin Hamiltonian parameters for $[\mathbf{1}]^+$ were undertaken using the B3LYP and PBE0 functionals, however, the relatively high level of spin contaminations (20 – 36%) in these calculations, as revealed by $\langle S^2 \rangle$ (Table S2), suggests that the spin Hamiltonian parameters calculated with these functionals are not reliable. Therefore we chose to compare the experimental spin Hamiltonian parameters with those calculated with the BP86 functional. Similar levels of spin contamination have been reported previously in calculations on the Ni-L state of the

[NiFe] hydrogenases and consequently interpretations were based on the results of calculations employing the BP86 functional.[17] We note that the calculated principal values of the hyperfine coupling constants for N(5) and N(6) are *ca.* $1 - 2 \times 10^{-4}$ cm^{-1} (Table S2) which is within the linewidth of the experimental spectrum (Figure 3a) and consequently these couplings are not resolved experimentally. Visualization of structures and isosurface plots of electronic properties were obtained with the program Molekel (version 5.4.0.8)[18] and Mayer bond orders and NAO analyses were carried out using the programs Multiwfn[19] and NBO 3.1.[20] Models of $[\mathbf{1}]^{2+}$ and $[\mathbf{1}]^{+}$ were constructed using geometrical data from the X-ray crystal structure of $[\mathbf{1}](PF_6)_2$. The co-ordinate frame employed in the calculations is shown in Figure 2. The x axis bisects the S(1)-Ni(1)-S(2) angle and the y axis lies in the plane defined by N(5)-Ni(1)-S(1).

X-ray crystallography Crystals of $[\mathbf{1}](PF_6)_2 \cdot MeCN$ were examined on a GV1000 Atlas CCD diffractometer using mirror-monochromated CuKα radiation (λ = 1.5418 Å). Intensities were integrated from data recorded on 1° frames by ω rotation. Cell parameters were refined from the observed positions of all strong reflections in each data set. A Gaussian grid face-indexed absorption correction with a beam profile correction was applied. The structures were solved by direct methods and were refined by full-matrix least-squares on all unique F^2 values, with anisotropic displacement parameters for all non-hydrogen atoms, and with constrained riding hydrogen geometries; U_{iso}(H) was set at 1.2 (1.5 for methyl groups) times U_{eq} of the parent atom. CrysAlisPro[21] (control and integration), and SHELX[22] and OLEX2[23] were employed for structure solution and refinement and for molecular graphics. Enhanced rigid bond restraints were applied to the thermal parameters of the CH_3CN atoms and to the atoms of the tert-butyl group defined by atoms C(17)-C(21). One of the two PF_6^- anions was disordered over two orientations hinging on the central P atom. The occupancies of the two conformations were refined competitively converging to a ratio of 0.29:0.71.
Enhanced rigid bond restraints were applied to the thermal parameters of the disordered PF_6^-.

References:

1. F. Osterloh, W. Saak and S. Pohl, *J. Am. Chem. Soc.*, 1997, **119**, 5648–5656.

2. G. E. S. M. J. Frisch, G. W. Trucks, H. B. Schlegel, T. V. M. A. Robb, J. R. Cheeseman, J. A. Montgomery, Jr., J. T. K. N. Kudin, J. C. Burant, J. M. Millam, S. S. Iyengar, N. R. V. Barone, B. Mennucci, M. Cossi, G. Scalmani, K. T. G. A. Petersson,

H. Nakatsuji, M. Hada, M. Ehara, O. K. R. Fukuda, J. Hasegawa, M. Ishida, T. Nakajima, Y. Honda, J. B. C. H. Nakai, M. Klene, X. Li, J. E. Knox, H. P. Hratchian, R. E. S. V. Bakken, C. Adamo, J. Jaramillo, R. Gomperts, J. W. O. O. Yazyev, A. J. Austin, R. Cammi, C. Pomelli, J. J. D. P. Y. Ayala, K. Morokuma, G. A. Voth, P. Salvador, M. C. S. V. G. Zakrzewski, S. Dapprich, A. D. Daniels, K. R. O. Farkas, D. K. Malick, A. D. Rabuck, S. C. J. B. Foresman, J. V. Ortiz, Q. Cui, A. G. Baboul, P. P. J. Cioslowski, B. B. Stefanov, G. Liu, A. Liashenko, M. A. A.-L. I. Komaromi, R. L. Martin, D. J. Fox, T. Keith, P. M. W. G. C. Y. Peng, A. Nanayakkara, M. Challacombe and and J. A. P. B. Johnson, W. Chen, M. W. Wong, C. Gonzalez, *Gaussian, Inc., Wallingford CT*, 2004.

3. A. D. Becke, *Phys. Rev. A*, 1988, **38**, 3098–3100.

4. J. Perdew, *Phys. Rev. B*, 1986, **33**, 8822–8824.

5. A. D. Becke, *J. Chem. Phys.*, 1993, **98**, 5648–5652.

6. C. Lee, W. Yang and R. G. Parr, *Phys. Rev. B*, 1988, **37**, 785–789.

7. A. Pardo, A. L. De Lacey, V. M. Fernández, H.-J. Fan, Y. Fan and M. B. Hall, *J. Biol. Inorg. Chem.*, 2006, **11**, 286–306.

8. P. J. Hay and W. R. Wadt, *J. Chem. Phys.*, 1985, **82**, 299-310.

9. M. Couty and M. B. Hall, *J. Comput. Chem.*, 1996, **17**, 1359–1370.

10. A. W. Ehlers, M. Biihme, S. Dapprich, A. Gobbi, A. Hijllwarth, V. Jonas, K. F. Kiihler, R. Stegmann, A. Veldkamp and G. Frenking, *Chem. Phys. Lett.*, 1993, **208**, 111–114.

11. C. E. Check, T. O. Faust, J. M. Bailey, B. J. Wright, T. M. Gilbert and L. S. Sunderlin, *J. Phys. Chem. A*, 2001, **105**, 8111–8116.

12. R. S. Grev and H. F. I. I. I. Schaefer, *J. Chem. Phys.*, 1989, **91**, 7305–7306.

13. C. W. Bauschlicher, S. R. Langhoff, H. Partridge and L. A. Barnes, *J. Chem. Phys.*, 1989, **91**, 2399- 2411.

14. R. Krishnan, J. S. Binkley, R. Seeger and J. A. Pople, *J. Chem. Phys.*, 1980, **72**, 650-654.

15. A. D. McLean and G. S. Chandler, *J Chem Phys*, 1980, **72**, 5639–5648.

16. V. Barone, in Recent Advances in Density Functional Methods, Part I, Ed. D. P. Chong World Scientific Publ. Co., Singapore, 1996.

17. M. Kampa, M.-E. Pandelia, W. Lubitz, M. van Gastel and F. Neese, *J. Am. Chem. Soc.*, 2013, **135**, 3915-3925.

18. S. Portmann and H. P. Lüthi, *Chimia (Aarau).*, 2000, **54**, 766–770.

19. T. Lu, F. Chen, *J. Comp. Chem*., 2012, **33**, 580-592.

20. NBO Version 3.1, E. D. Glendening, A. E. Reed, J. E. Carpenter, and F. Weinhold.

21. *CrysAlis PRO*, Agilent Technologies, Yarnton, England 2010.

22. G. M. Sheldrick, *SHELXTL Acta Crystallogr*., *Sect*. *A* 2008, **64**, 112-122.

23. O. V. Dolomanov, L. J. Bourhis, R. J. Gildea, J. A. K. Howard, H. Puschmann, *Olex2 J*. *Appl*. *Cryst*. 2009, **42**, 339-341.

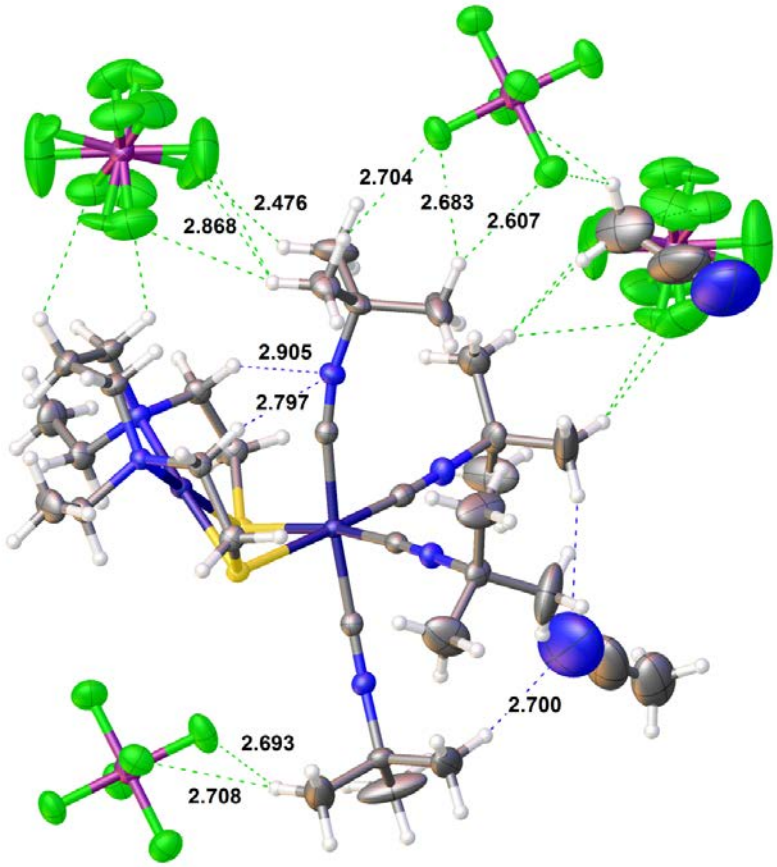

Figure S1: Expansion of the short contacts in the X-ray crystal structure of [**1**]$(PF_6)_2$·MeCN.

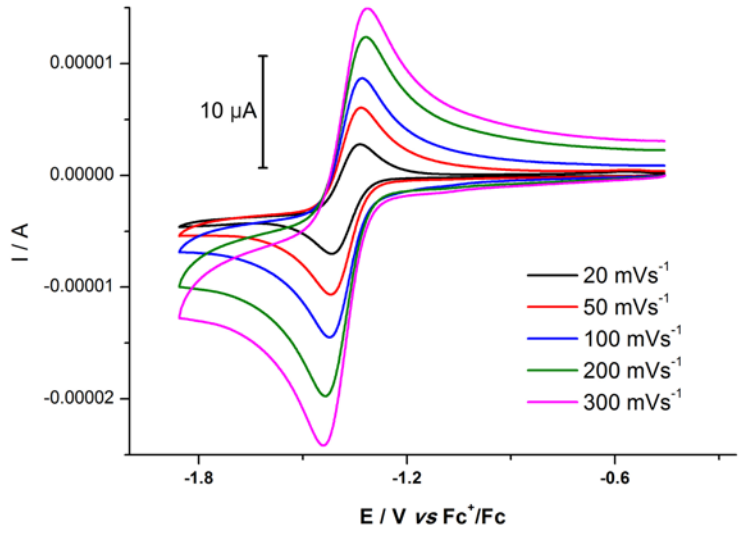

Figure S2: Cyclic voltammograms of [**1**]$(PF_6)_2$ (1 mM) in MeCN / 0.2 M $[N^nBu_4][BF_4]$ at various scan rates at 298 K.

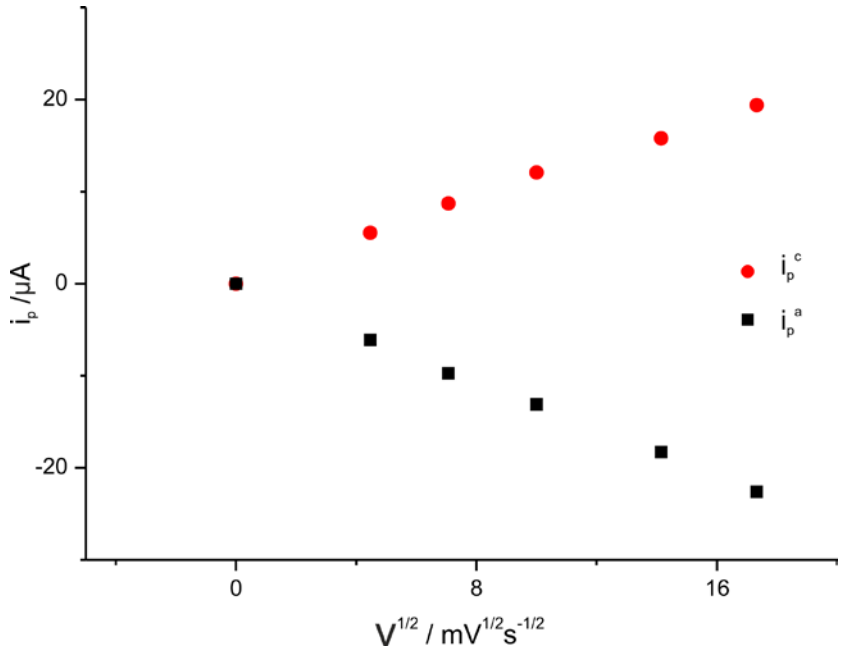

Figure S3: Plot of I_p *vs* $v^{1/2}$ for the reversible reduction process at *ca.* −1.39 V vs Fc^+/Fc for [**1**]$(PF_6)_2$ at 298 K.

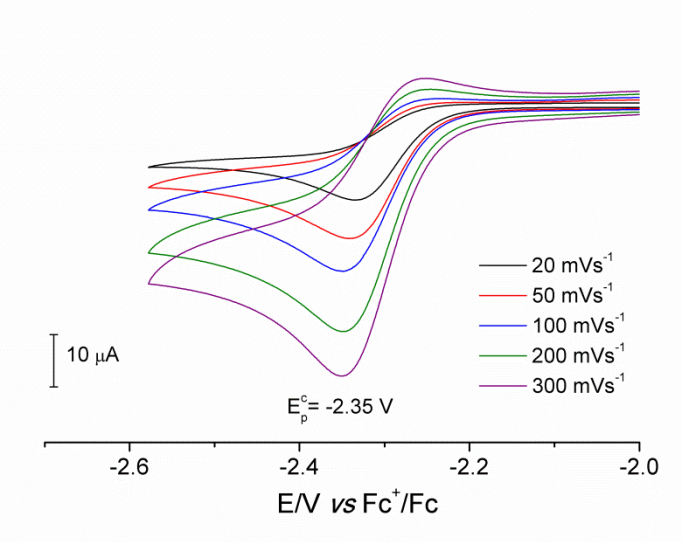

Figure S4: Cyclic voltammograms of [Ni(L^1)] (1 mM) in MeCN / 0.2 M [N^nBu_4][BF_4] at various scan rates at 298 K.

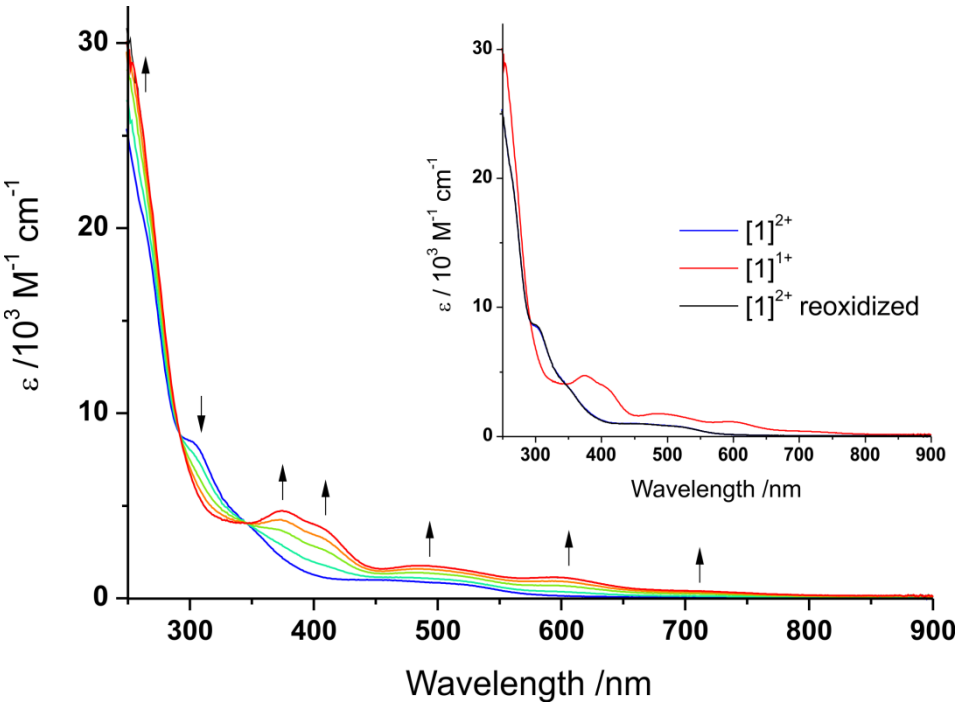

Figure S5: Electronic spectra for the reduction of a 2 mM solution of [**1**]$(PF_6)_2$ in MeCN / 0.2 M [N^nBu_4][BF_4] at 243 K. Inset, UV/vis spectra of [**1**]$(PF_6)_2$ before reduction, after reduction and after complete reoxidation.

Table S1: UV/vis absorbances of [**1**]$(PF_6)_2$ and [**1**]$^+$ generated from [**1**]$(PF_6)_2$ in MeCN / 0.2 M [N^nBu_4][BF_4] at 243 K.

	[1]$^{2+}$	**[1]$^{1+}$**	**Isosbestic Point**
λ_{max} / nm (ε / $M^{-1}cm^{-1}$)	219 (30500), 247 (25900), 266 (19000), 305 (8300), 350 (3800), 450 (1000), 520 (750)	230 (31300), 375 (4700), 400 (3900), 490 (1760), 520 (1500), 598 (1100), 720 (380)	346 (4000)

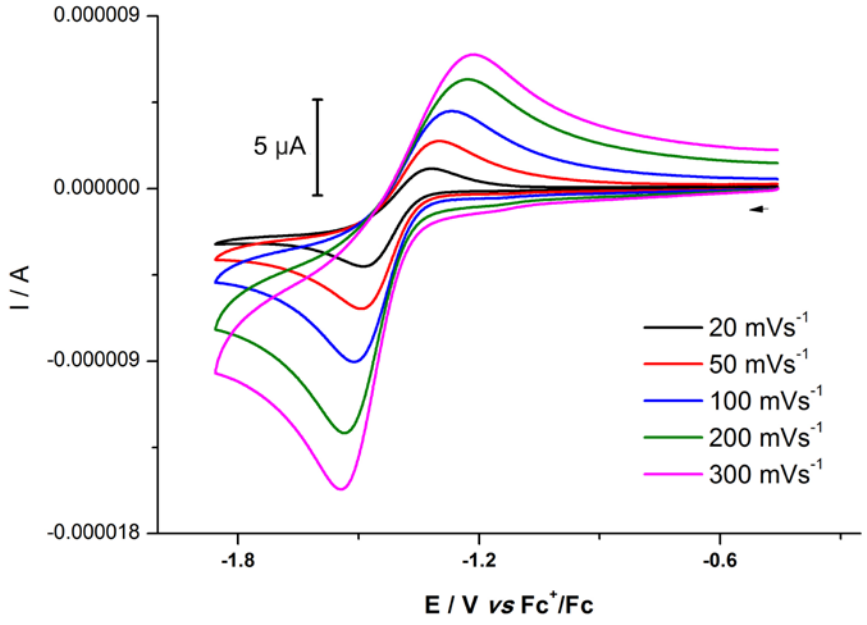

Figure S6: Cyclic voltammograms of [**1**]$(PF_6)_2$ (1 mM) in MeCN / 0.2 M [N^nBu_4][BF_4] at various scan rates at 243 K.

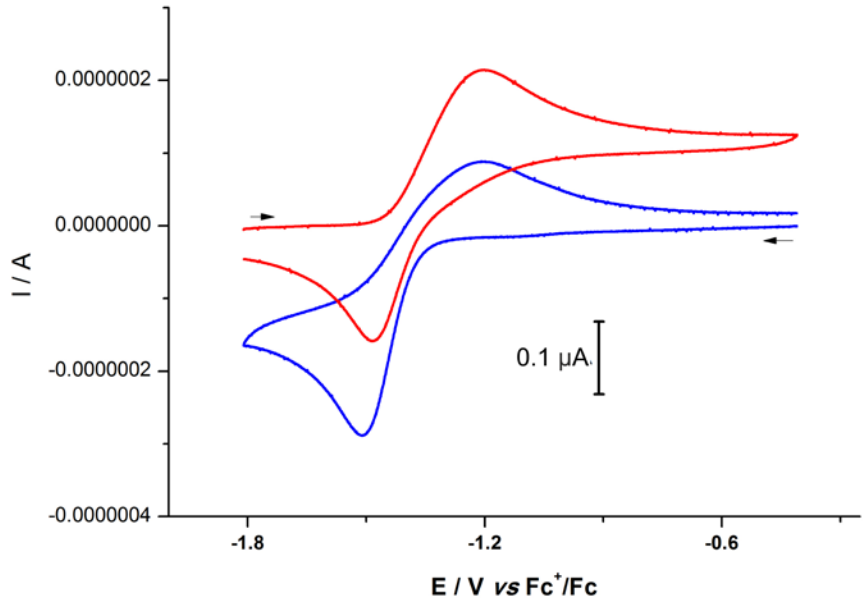

Figure S7: Cyclic voltammograms of [**1**]$(PF_6)_2$ (0.93 mM) in MeCN / 0.2 M [N^nBu_4][BF_4] at 243 K before (blue line) and after bulk electrochemical reduction (red line). The difference in response before and after bulk electrochemical reduction results from the change in resting state following the bulk reduction of a solution containing oxidised material.

Table S2: Spin Hamiltonian parameters for $[\mathbf{1}]^+$ from the simulation of the X-band EPR spectrum of $[\mathbf{1}]^+$ as a solution in MeCN / 0.2 M $[N^nBu_4][BF_4]$ at 77 K and from gas-phase unrestricted BP86 DFT calculations on a model of $[\mathbf{1}]^+$.

	Principal *g*-values			Linewidth /G				^{14}N hyperfine /x 10^{-4} cm^{-1}		
	g_{11}	g_{22}	g_{33}	W_{11}	W_{22}	W_{33}		a_1	a_2	a_3
Experimental	2.210	2.074	2.074	18	16	17		unresolved		
BP86	2.174	2.079	2.070				N(5)	-1.048	-1.005	2.196
$<S^2> = 0.77$							N(6)	-1.054	-1.012	2.210
PBE0	2.287	2.207	2.196				N(5)	-0.907	-0.860	1.767
$<S^2> = 1.02$							N(6)	-0.910	-0.864	1.775
B3LYP	2.267	2.165	2.156				N(5)	-0.931	-0.887	1.818
$<S^2> = 0.90$							N(6)	-0.935	-0.891	1.826

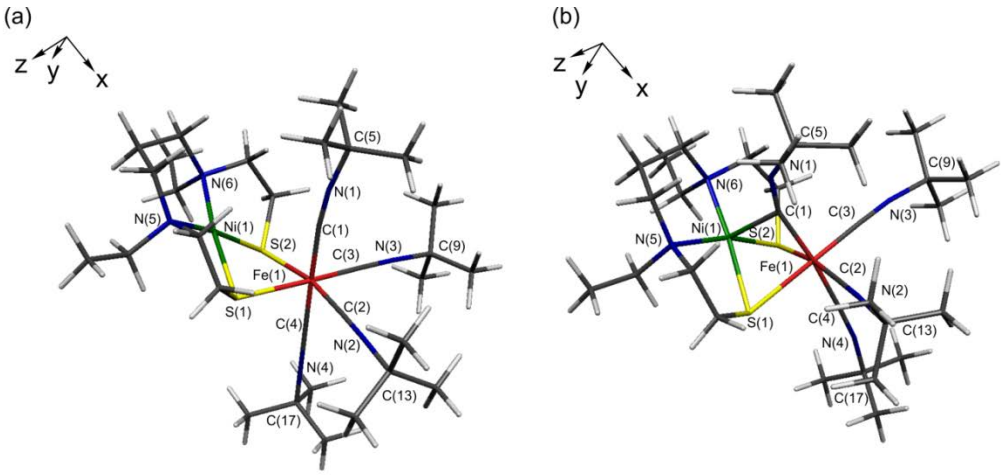

Figure S8: The gas-phase optimized structures of (a) $[\mathbf{1}]^{2+}$ and (b) $[\mathbf{1}]^+$ derived from DFT calculations**.**

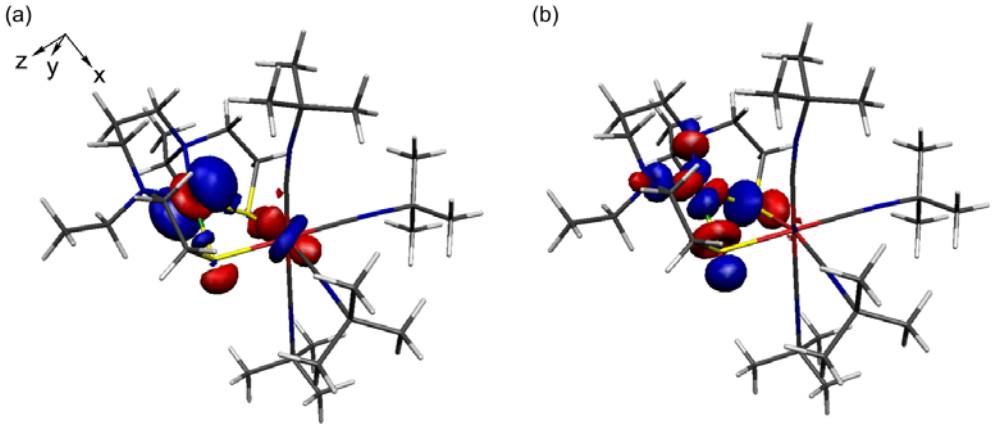

Figure S9: (a) Kohn-Sham HOMO and (b) Kohn-Sham LUMO for the gas-phase geometry optimized structure of $[\mathbf{1}]^{2+}$ plotted at an isosurface value of 0.05 eÅ^{-3}.

Table S2: Selected metrical parameters for $[\mathbf{1}]^{2+}$ in the X-Ray structure of $[\mathbf{1}](PF_6)_2 \cdot MeCN$ and for the gas-phase geometry optimized structures of $[\mathbf{1}]^{2+}$ and $[\mathbf{1}]^{+}$.

Distances (Å) /	$[\mathbf{1}]^{2+}$		$[\mathbf{1}]^{+}$
angles (deg.)	X-ray	BP86	BP86
Ni(1)-Fe(1)	2.9896(4)	3.209	2.616
Ni(1)-C(1)	2.951(2)	3.234	2.018
Ni(1)-S(1)	2.1704(5)	2.219	2.357
Ni(1)-S(2)	2.1784(5)	2.220	2.356
Ni(1)-N(5)	1.986(2)	2.018	2.130
Ni(1)-N(6)	1.984(2)	2.027	2.130
Fe(1)-S(1)	2.3371(5)	2.386	2.434
Fe(1)-S(2)	2.3195(5)	2.388	2.433
Fe(1)-C(1)	1.890(2)	1.864	1.942
Fe(1)-C(2)	1.859(2)	1.835	1.808
Fe(1)-C(3)	1.870(2)	1.834	1.809
Fe(1)-C(4)	1.888(2)	1.882	1.862
S(1)-Ni(1)-S(2)	81.76(2)	82.1	85.2
N(5)-Ni(1)-N(6)	101.11(7)	102.0	99.0
S(1)-Fe(1)-S(2)	75.35(2)	75.3	81.9
C(1)-Fe(1)-C(4)	173.60(8)	178.8	173.4
C(2)-Fe(1)-C(3)	96.79(8)	94.7	95.9
Fe(1)-C(1)-N(1)	170.0(2)	173.7	157.2
Fe(1)-C(2)-N(2)	175.3(2)	178.5	178.0
Fe(1)-C(3)-N(3)	175.1(2)	178.8	177.5
Fe(1)-C(4)-N(4)	172.9(2)	179.3	178.1
C(1)-N(1)-C(5)	166.5(2)	170.7	140.9
C(2)-N(2)-C(13)	177.7(2)	176.8	169.3
C(3)-N(3)-C(13)	176.6(2)	177.5	171.5
C(4)-N(4)-C(17)	168.2(2)	180.0	170.1
$Ni(1)S_2/Fe(1)S_2$	117.94(3)	128.3	94.1

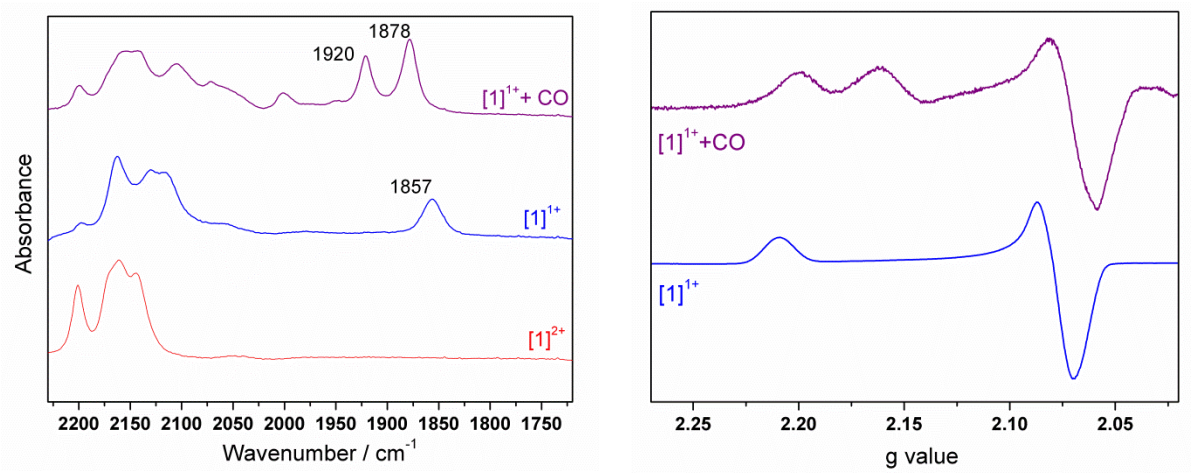

Figure S10: Left: solution IR spectra (MeCN) of [**1**]$(PF_6)_2$ before chemical reduction (red), after reduction (blue) and after reaction with CO (purple). Right: frozen EPR spectra of [**1**]$^{1+}$ and of the reaction mixture obtained by passing CO gas through the MeCN solution of [**1**]$^{1+}$.

Table S3: Cartesian coordinates for the optimized geometry of $[\mathbf{1}]^{2+}$.

Energy (B3LYP) = -5114.42465124 h

Ni	-0.00000	0.00000	0.00000
Fe	2.84529	0.02790	-1.48347
S	1.67326	1.45698	0.02538
S	1.67445	-1.45698	-0.02538
N	0.83910	0.09996	-3.77443
N	4.34548	2.28863	-2.80319
N	4.33295	-2.15350	-2.94261
N	4.99963	-0.04061	0.68990
N	-1.27092	1.56707	-0.02538
N	-1.27328	-1.57602	-0.04155
C	1.55919	0.07560	-2.83188
C	0.15113	0.12829	-5.06236
C	-0.64448	1.45019	-5.16131
H	-1.42247	1.51104	-4.37754
H	-1.14924	1.49924	-6.14420
H	0.02479	2.32666	-5.07576
C	-0.79543	-1.09162	-5.13762
H	-0.23423	-2.04006	-5.04247
H	-1.30904	-1.09461	-6.11716
H	-1.56997	-1.04790	-4.34896
C	1.23073	0.05495	-6.16863
H	1.92269	0.91504	-6.10304
H	0.74000	0.07834	-7.15946
H	1.81397	-0.88141	-6.09195
C	3.74954	1.39846	-2.30266
C	5.14046	3.37365	-3.36702
C	6.48734	2.77587	-3.83781
H	7.03831	2.32343	-2.99250
H	7.11189	3.58193	-4.26580
H	6.33129	2.00794	-4.61805
C	5.35827	4.42657	-2.25495
H	4.39579	4.84196	-1.90253
H	5.96601	5.25876	-2.65653
H	5.89588	3.98994	-1.39316
C	4.35613	3.97566	-4.55571
H	4.18348	3.21865	-5.34316
H	4.94414	4.80183	-4.99663
H	3.38285	4.38474	-4.22682
C	3.73811	-1.29960	-2.38100
C	5.12065	-3.17875	-3.61728
C	4.14425	-4.13993	-4.33512
H	3.46859	-4.63577	-3.61350
H	4.72497	-4.92482	-4.85438
H	3.53891	-3.60451	-5.09015
C	5.94449	-3.92681	-2.54305
H	6.63597	-3.23835	-2.02277

H	6.54536	-4.71621	-3.03172
H	5.28600	-4.40675	-1.79499
C	6.04645	-2.46810	-4.63262
H	5.45845	-1.91368	-5.38775
H	6.65824	-3.22542	-5.15717
H	6.72990	-1.76498	-4.12106
C	4.17112	-0.00569	-0.14813
C	6.02403	-0.08479	1.72621
C	5.39139	0.46474	3.02624
H	5.05428	1.51006	2.89297
H	6.14495	0.44150	3.83502
H	4.52701	-0.15225	3.33662
C	7.20568	0.79712	1.26121
H	7.63521	0.42164	0.31354
H	7.99785	0.77420	2.03253
H	6.88777	1.84745	1.12479
C	6.45705	-1.55952	1.89620
H	5.59938	-2.19355	2.19057
H	7.22268	-1.62206	2.69166
H	6.89471	-1.95748	0.96197
C	0.76095	2.91954	-0.68849
H	0.82005	3.71805	0.07715
H	1.28795	3.27395	-1.59301
C	-0.67665	2.53416	-1.02509
H	-1.31947	3.43745	-1.10316
H	-0.69564	2.01588	-2.00102
C	-1.28296	2.13801	1.38715
H	-0.22631	2.24708	1.69443
H	-1.70705	1.34895	2.03548
C	-2.03572	3.46184	1.59820
H	-1.63253	4.28953	0.98557
H	-1.90554	3.75475	2.65813
H	-3.12390	3.38588	1.42097
C	-2.66940	1.26517	-0.48155
H	-2.63655	1.15171	-1.58295
H	-3.31033	2.14276	-0.26562
C	-3.28056	-0.00130	0.12282
H	-3.23413	0.00293	1.22990
H	-4.36108	0.00219	-0.12780
C	-2.68313	-1.27881	-0.47060
H	-3.32144	-2.15033	-0.22421
H	-2.67731	-1.18722	-1.57436
C	-1.26374	-2.16564	1.36188
H	-1.71784	-1.39989	2.01874
H	-0.20383	-2.24176	1.66787
C	-1.96743	-3.51901	1.55547
H	-3.05327	-3.48857	1.35080
H	-1.85083	-3.80776	2.61806
H	-1.51545	-4.32815	0.95213
C	-0.68747	-2.51856	-1.06818

H	-0.72464	-1.97671	-2.03067
H	-1.32658	-3.42368	-1.15562
C	0.75608	-2.90438	-0.76106
H	1.26970	-3.24054	-1.68048
H	0.82877	-3.71764	-0.01223

Table S4: Cartesian coordinates for the optimized geometry of [**1**]$^{+}$.

Energy (B3LYP) = -5114.64496284 h

Ni	-0.00000	0.00000	0.00000
Fe	1.86615	-0.25496	-1.81586
S	1.73585	1.57899	-0.22086
S	1.73387	-1.57899	0.22086
N	-1.12598	-0.32132	-2.57897
N	2.24731	1.65376	-4.09586
N	2.25978	-2.75609	-3.42111
N	4.83672	-0.14802	-1.14863
N	-1.31078	1.66416	0.22086
N	-1.31290	-1.54455	0.65254
C	-0.04651	-0.26655	-1.99944
C	-1.69353	-0.43662	-3.93948
C	-2.02398	0.99255	-4.43025
H	-2.74740	1.48912	-3.75674
H	-2.47154	0.95071	-5.44074
H	-1.10646	1.60912	-4.47952
C	-2.98736	-1.27691	-3.84816
H	-2.77201	-2.29530	-3.47313
H	-3.45103	-1.37204	-4.84733
H	-3.72364	-0.80163	-3.17334
C	-0.68379	-1.11361	-4.89182
H	0.25422	-0.53084	-4.94731
H	-1.11768	-1.18945	-5.90628
H	-0.43663	-2.13086	-4.53746
C	2.07099	0.89545	-3.19553
C	2.72485	2.55222	-5.13001
C	3.51244	1.71392	-6.16635
H	4.37274	1.20914	-5.68827
H	3.89437	2.37457	-6.96626
H	2.86327	0.94640	-6.62747
C	3.64454	3.60522	-4.46575
H	3.09250	4.18986	-3.70655
H	4.02623	4.30283	-5.23384
H	4.50642	3.11800	-3.97338
C	1.50562	3.23350	-5.79468
H	0.83845	2.48391	-6.25912
H	1.85200	3.92501	-6.58446
H	0.92594	3.81604	-5.05495
C	2.07461	-1.76105	-2.79659

C	2.69485	-3.93779	-4.13912
C	1.58149	-5.00841	-4.04651
H	1.38784	-5.28647	-2.99394
H	1.89484	-5.91756	-4.59174
H	0.64001	-4.64213	-4.49585
C	3.99844	-4.44752	-3.47830
H	4.79116	-3.67843	-3.53347
H	4.35147	-5.35470	-4.00240
H	3.82835	-4.70005	-2.41493
C	2.94735	-3.54052	-5.61379
H	2.02316	-3.15406	-6.08210
H	3.28442	-4.42525	-6.18448
H	3.73023	-2.76217	-5.68037
C	3.68730	-0.19334	-1.43176
C	6.16251	-0.04370	-0.56992
C	5.99646	0.03346	0.96657
H	5.39402	0.91781	1.24955
H	6.99015	0.11234	1.44418
H	5.48747	-0.87117	1.35069
C	6.82520	1.24151	-1.11965
H	6.92516	1.19540	-2.22011
H	7.83378	1.35395	-0.68147
H	6.22619	2.13284	-0.85315
C	6.96794	-1.29952	-0.97826
H	6.47716	-2.21746	-0.60404
H	7.98301	-1.24460	-0.54414
H	7.06161	-1.36871	-2.07807
C	0.63663	2.99912	-0.71907
H	0.82537	3.77674	0.04813
H	0.97386	3.40751	-1.68986
C	-0.85629	2.64686	-0.81459
H	-1.46134	3.57816	-0.76031
H	-1.05521	2.17347	-1.79179
C	-1.12487	2.20397	1.61424
H	-0.03581	2.34360	1.75031
H	-1.41395	1.39809	2.31279
C	-1.88182	3.49690	1.97365
H	-1.58576	4.35224	1.33867
H	-1.63371	3.76667	3.01769
H	-2.98000	3.38217	1.91799
C	-2.73267	1.30264	-0.06063
H	-2.77876	1.05730	-1.13931
H	-3.38708	2.18360	0.11098
C	-3.27588	0.09970	0.72991
H	-3.16170	0.24547	1.82160
H	-4.37027	0.07641	0.55187
C	-2.73331	-1.26887	0.28253
H	-3.38910	-2.07342	0.67817
H	-2.77797	-1.31647	-0.82269
C	-1.13165	-1.69975	2.13938

H	-1.42635	-0.74012	2.60115
H	-0.04291	-1.79430	2.31165
C	-1.88686	-2.85611	2.82221
H	-2.98506	-2.76481	2.73337
H	-1.64369	-2.84129	3.90156
H	-1.58480	-3.84684	2.43535
C	-0.85529	-2.76429	-0.08747
H	-1.04518	-2.56136	-1.15627
H	-1.46408	-3.64817	0.20314
C	0.63551	-3.08030	0.11056
H	0.97937	-3.73167	-0.71416
H	0.81543	-3.62640	1.05835